Proceedings of the 28th IEEE
EMBS Annual International Conference
New York City, USA, Aug 30-Sept 3, 2006

An Efficient MR Image Reconstruction Method for Arbitrary K-space Trajectories Without Density Compensation

Jiayu Song*, *Student Member, IEEE* and Qing H. Liu, *Fellow, IEEE*

Abstract— **Non-Cartesian sampling is widely used for fast magnetic resonance imaging (MRI). The well known gridding method usually requires density compensation to adjust the non-uniform sampling density, which is a major source of reconstruction error. Minimum-norm least square (MNLS) reconstruction, on the other hand, does not need density compensation, but requires intensive computations. In this paper, a new version of MNLS reconstruction method is developed using maximum likelihood and is speeded up by incorporating novel non-uniform fast Fourier transform (NUFFT) and bi-conjugate gradient fast Fourier transform (BCG-FFT) techniques. Studies on computer-simulated phantoms and a physically scanned phantom show improved reconstruction accuracy and signal-to-noise ratio compared to gridding method. The method is shown applicable to arbitrary k-space trajectory. Furthermore, we find that the method in fact performs un-blurring in the image space as an equivalent of density compensation in the k-space. Equalizing MNLS solution with gridding algorithm leads to new approaches of finding optimal density compensation functions (DCF). The method has been applied to radially encoded cardiac imaging on small animals. Reconstructed dynamic images of an in vivo mouse heart are shown.**

I. INTRODUCTION

In magnetic resonance imaging (MRI), the recorded signal in the spatial-frequency space (known as k-space) is proportional to the Fourier transform of the transverse magnetization. Non-Cartesian trajectories, such as radial and spiral, have recently gained increased attention in various applications including functional brain imaging, hyperpolarized gas imaging, contrast-enhanced MR angiography and cardiac imaging. High-fidelity image reconstruction from these non-Cartesian samples is challenging. The existing reconstruction methods generally fall in two categories: gridding reconstruction and minimum-norm least square reconstruction.

Both data-driven and grid-driven gridding methods [1][2][3][4] first interpolate the non-Cartesian samples to Cartesian grid and then use FFT. The data-driven gridding method [1][2] convolves interpolation kernels with each non-Cartesian sample, and it requires a pre-weighting (also called density compensation) on the raw data to compensate for the non-uniform sampling density. Density compensation functions (DCF) can be determined by Jacobian [5], convolution of delta functions located at k-samples with the interpolation kernel [2], analytical solutions [6] or Voronoi diagram [7]. Unfortunately, a mathematically ideal DCF usually does not provide highest image quality. Pipe *et al.* [8] suggested an iterative approach to find DCF that satisfies necessary conditions. On the other hand, grid-driven gridding methods such as URS/BURS [3] find interpolation window for each resampled Cartesian nodes by inverting the interpolation coefficient matrix. Relating the grid-driven method and the data-driven method, Sedarat *et al.* [4] suggested to find optimal DCF through matrix approximation and singular value decomposition (SVD), but the computational cost is still intense.

Alternatively, minimum-norm least square methods try to minimize the energy of the reconstruction error. Walle *et al.* [9] introduced a continuous to discrete mapping concept and utilized SVD to compute the Moore-Penrose pseudoinverse. The complexity is significant, which limits it to applications with small number of samples. Nevertheless, the inversion needs to be performed only once for a given sampling pattern, and in fact, that inverted matrix contains the exact DCF. The normal DCF used in data-driven gridding methods is only an approximation of its diagonal.

Different from [9], this work uses a different version of least square formulation derived using maximum likelihood theory. Due to the block Toeplitz nature of the matrix to be inverted, it can be computed efficiently using iterative method. BCG-FFT method [10] and NUFFT [11][12] are utilized to reduce the computational complexity. This Toeplitz Maximum Likelihood (TML) method is an extension of the idea of Liu *et al*'s 1D non-uniform inverse fast Fourier transform (NUIFFT) [13] and we noticed similar ideas had been mentioned very recently by [14] and [15] in their iterative reconstruction algorithms. This formulation does not require a DCF, and thus is generally applicable to arbitrary k-space trajectory. We also discuss the physical interpretation of this method and show that the initial no-density-compensated image is sharpened during each iteration by the un-blurring matrix. This indicates that compensating the sampling density in the k-space (e.g. gridding method) is equivalent to un-blurring the reconstructed image in the image space. Based on that, alternative approaches to optimize DCF are suggested. The developed TML method is compared to the regular density compensated gridding methods on computer simulation studies, as well as physical scans.

II. TOEPLITZ MAXIMUM LIKELIHOOD METHOD

The discretized MRI signal model without considering field inhomogeneity or sensitivity is

$$s(\mathbf{k}_m) \approx \sum_{\mathbf{x}} I(\mathbf{x}) e^{-i2\pi \mathbf{k}_m \cdot \mathbf{x}} + \mathcal{N}_s(\mathbf{k}_m) \qquad (1)$$

Jiayu Song is with Department of Electrical & Computer Engineering, Duke University, Durham, NC 27708, and the Center for In Vivo Microscopy, Duke University Medical Center, Durham, NC 27710. jiayu.song@duke.edu

Dr. Qing H. Liu is with Department of Electrical & Computer Engineering, Duke University, Durham, NC 27708. qhliu@duke.ee.edu

where M_{xy} (equivalent to the image I) is the transverse magnetization in d-dimensional spatial domain $\mathbf{x}$, $\mathbf{k}$ is the k-space trajectory, and $\mathcal{N}_s(\mathbf{k})$ is the measurement noise. A compact version of (1) becomes

$$\underline{\mathbf{s}} = A\underline{\mathbf{i}} + \underline{\mathbf{n}}_s \tag{2}$$

Where $\underline{\mathbf{s}}$ and $\underline{\mathbf{i}}$ are s and I aligned as vectors, and A is the system transfer matrix with elements $a_{n,m} = e^{-i2\pi\mathbf{k}_m\cdot\mathbf{x}_n}$.

Assuming the measurement noise in MRI is independent and has Gaussian distribution, the probability density function of the noise is therefore given by

$$P(\underline{\mathbf{n}}_s) = \left(\frac{1}{2\pi\sigma_s^2}\right)^M e^{-\left((\underline{\mathbf{s}}-A\underline{\mathbf{i}})^\dagger(\underline{\mathbf{s}}-A\underline{\mathbf{i}})\right)/2\sigma_s^2} \tag{3}$$

where M is the total number of k-space samples. Likelihood maximization of (3) leads to minimum-norm least square solutions

$$\underline{\mathbf{i}}_{ML} = A^\dagger\left(AA^\dagger\right)^{-1}\underline{\mathbf{s}}, \tag{4}$$

or

$$\underline{\mathbf{i}}_{ML} = \left(A^\dagger A\right)^{-1}A^\dagger\underline{\mathbf{s}} \tag{5}$$

Note (4) is the formula version used by [9]. Matrix operator $AA^\dagger$ has the dimension of sample number, and its elements have closed-form expressions. However, either solving it by pseudoinverse or iterative methods involves intensive computations. In contrast, in this paper, we use the second formula version (5). The direct inversion of $A^\dagger A$ is prohibitively expensive for large image sizes and in high dimensions. However, it is noticed that $A^\dagger A$ is a block-Toeplitz matrix and its element can be written as

$$\left(A^\dagger A\right)_{p,q} = \sum_m e^{i2\pi\mathbf{k}_m\cdot(\mathbf{x_{np}}-\mathbf{x_{nq}})} = \alpha_{\mathbf{np}-\mathbf{nq}} \tag{6}$$

where $\mathbf{np},\mathbf{nq} \in (-N_d/2, N_d/2-1)^d$. Furthermore, we define $\alpha_{-\mathbf{n}} = \alpha_{\mathbf{n}}^*$, so that another half of the elements calculation is saved. As a result, only $2\prod_{p=1}^{d} N_p$ elements out of $\prod_{p=1}^{d}(N_p)^2$ are independent, and they can be efficiently calculated with NUFFT-2 [16].

$$\underline{\mathbf{g}} = A^\dagger\underline{\mathbf{s}} = \sum_m \underline{\mathbf{s}}(\mathbf{k}_m)e^{i2\pi\mathbf{k}_m\cdot\mathbf{x}} \tag{7}$$

(7) can also be evaluate efficiently using d-dimensional NUFFT-2 and $\underline{\mathbf{i}}_{ML}$ will then be obtained by solving

$$\underline{\mathbf{g}}_{\mathbf{np}} = \sum_{\mathbf{nq}} \alpha_{\mathbf{np}-\mathbf{nq}} I_{\mathbf{nq}} = \mathscr{F}^{-1}(\mathscr{F}(\alpha)\mathscr{F}(I)) \tag{8}$$

iteratively. Bi-conjugate gradient method is used since $A^\dagger A$ is in general non-symmetric. In each iteration, the calculation of the convolution can be speeded up by regular d-dimensional FFT and IFFT. Note $A^\dagger A$ does not vary from iteration to iteration, thus the FFT of α needs to be calculated only once for all iterations. As a result, this Toeplitz based Maximum Likelihood (TML) reconstruction algorithm includes only two NUFFT-2 evaluations and several iterations of regular FFT and IFFT.

III. SIMULATION STUDY

A. One-Dimensional Case

We start the simulation study with 1D "image" $I(x)$ for better illustration of the algorithm. The spatial-frequency response s is sampled at M arbitrary locations $k_m = (m+v)/M, m = -M/2, 1, \cdots, M/2-1$, where v is a random number uniformly distributed in $(-0.5, 0.5)$. Notice this general non-Cartesian sampling pattern can result in very high non-uniformity, therefore violation of Nyquist criterion. The noise-free signal samples are calculated as

$$s(k_m) = \sum_n I(x_n)e^{-i2\pi k_m\cdot x_n}. \tag{9}$$

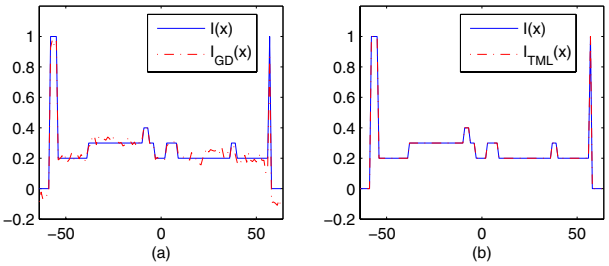

Fig. 1. Comparison of gridding method (a) and Toeplitz based maximum likelihood method (b) on a boxcar 1D phantom image.

Fig. 1 shows the reconstruction results using the proposed TML method (I_{TML}) and density compensated gridding method (I_{GD}). We formulated the density compensated gridding method as

$$I_{GD} = \sum_n \Delta k_m I(x_n)e^{i2\pi k_m\cdot x_n}. \tag{10}$$

In Fig. 1, the reconstruction errors, defined as $e_{L2} = \|I_{TML} - I\|_2/\|I\|_2$, are 16.16% for the gridding and 0.0013% for TML, respectively. The poor DCF estimation for the gridding method at such a high non-uniformity is the main source of error. In comparison, TML shows significant image quality improvement over gridding and the reconstruction takes only 0.08 second (CPU: AMD ATHLON 2600+) with 21 BCG-FFT iterations.

B. Two-Dimensional Case

In the 2D simulation study, we first implemented practical trajectories, including radial and spiral, on a Shepp-Logan phantom. 400 radial rays were simulated for a 128×128-sized phantom, and for spiral sampling, 16 interleaves were used. Fig. 2 shows the reconstruction results using gridding method and TML. In the gridding reconstruction, we used Jacobian DCF [5] for radial sampling and Voronoi DCF [7] for spiral sampling. The difference images are shown on a 1/10 grayscale. For radial sampling, the reconstruction errors are 3.20% for gridding and 0.05% for TML, which uses 31 BCG-FFT iterations. For spiral, the reconstruction errors are 6.54% for gridding and 2.86% for TML.

To demonstrate that the proposed method works for arbitrary k-space sampling while gridding method might not, we generated a 2D random sampling pattern comparable

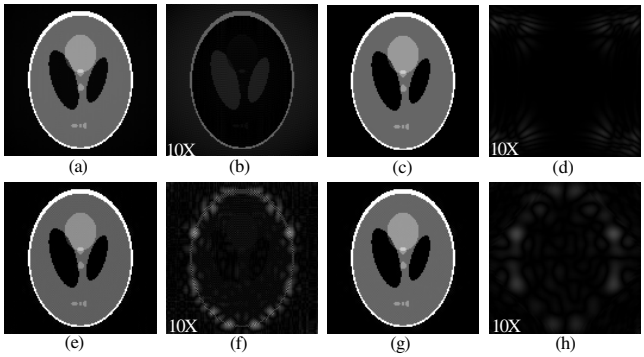

Fig. 2. Comparison of reconstruction results using gridding method and TML method on radial (a)(b)(c)(d) and spiral (e)(f)(g)(h) trajectories. (a)(e) $I_{GD}(\mathbf{x})$, (b)(f) $10\times|I_{GD}(\mathbf{x})-I(\mathbf{x})|$, (c)(g) $I_{TML}(\mathbf{x})$, (d)(h) $10\times|I_{TML}(\mathbf{x})-I(\mathbf{x})|$

to the 1D case. Fig. 3 shows the reconstructed image by TML method, the difference image, and the line profile. The reconstruction error is only 1.76%. It shows that the existence of DCF is no longer a limitation, which provides the potential to make the pulse sequence design more flexible and enable new trajectories. In this case, DCF cannot be easily found as "the area associated with each sample," so we did not include gridding method for comparison.

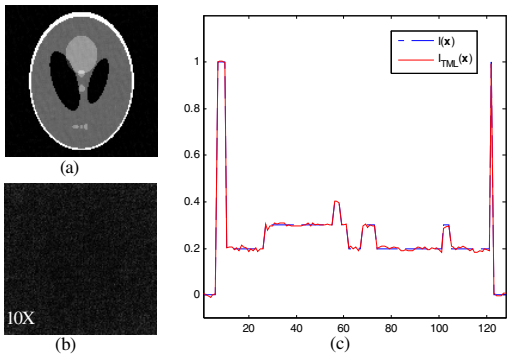

Fig. 3. TML reconstruction of a randomly sampled 2D Shepp-Logan phantom. (a) $I_{TML}(\mathbf{x})$, (b) $10\times|I_{TML}(\mathbf{x})-I(\mathbf{x})|$, (c) center line profile.

SNR	100	50	40	30
Gridding	3.19%	3.20%	6.72%	12.26%
TML(radial)	0.05%	0.27%	0.86%	2.73%
TML(random)	1.76%	1.80%	2.38%	6.62%

TABLE I

COMPARISON OF RECONSTRUCTION ERRORS USING GRIDDING METHOD AND TML AT DIFFERENT SNR LEVELS.

Reconstruction performance at the appearance of noise was also examined by adding Gaussian noise to the simulated *k*-space data. The reconstruction errors at different measurement signal-to-noise ratio (SNR) levels are summarized in Table. I. TML was applied to both radial and random samplings, and gridding method was only applied to radial sampling. We used linear scale for the SNR.

IV. PHYSICAL SCAN RESULTS

A. Phantom Scan

A cylindrical water tube phantom was scanned on a 2 Tesla GE Oxford horizontal magnet. 2D radial encoding spin-echo sequence was applied. We collected two data sets. One had 800 rays, which supports the Nyquist sampling rate, and the other had 200 rays, which corresponds to an azimuthally under-sampled case. Both data sets collected 186 samples on each ray. Fig. 4 shows the reconstructed images side by side. We measured the image SNR by

$$SNR_I = \frac{\langle I(x, x\in R_{obj})\rangle}{\sqrt{\frac{1}{M-1}\sum_{x_m\in R_{bkg}}\left(I(x_m)-\langle I(x, x\in R_{bkg})\rangle\right)^2}} \quad (11)$$

The well sampled case is of relatively higher SNR, and thus Fig. 4(a) and (b) have very similar visual qualities, though quantitatively TML reconstruction has an SNR 16.2% higher. In comparison, for the 200-ray data set, the TML generated image is visually better than the gridding one, and the SNR is 1.54 times higher. We use image (b) as the reference image and subtract it from images (c) and (d) to create difference images (e) and (f).

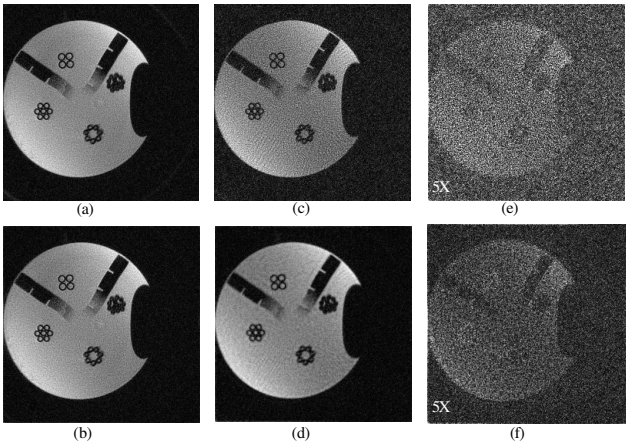

Fig. 4. Comparison of reconstructions using gridding and TML methods on a radial scan of a water phantom. (a) $I^{(1)}_{GD}$, 800 rays (b) $I^{(1)}_{TML}$, 800 rays (c) $I^{(2)}_{GD}$, 800 rays (d) $I^{(1)}_{TML}$, 200 rays, (e) $5\times|I^{(2)}_{GD}-I^{(1)}_{TML}|$, (f) $5\times|I^{(2)}_{TML}-I^{(1)}_{TML}|$.

B. In Vivo Scan

Fast non-Cartesian imaging technique has been favorably used for cardiac imaging due to robustness against motion and enhanced SNR. A 2D radially encoded data set was acquired of a live mouse using a gated acquisition on a 7T magnet[1]. 8 dynamic images recoding a cardiac cycle are acquired and 1800 rays were collected for each image frame. These images were reconstructed using the Toeplitz based maximum likelihood method and shown in Fig 5. Since these dynamic images have a strong temporal correlation, we actually use the first reconstructed image as the initial guess

[1]The authors would like to thank Elizabeth Bucholz and James Pollaro of the Duke center for in vivo microscopy for performing the cardiac scans.

of BCG-FFT iteration to speed up the rest reconstructions. This turns out to be another advantage of TML method over gridding method.

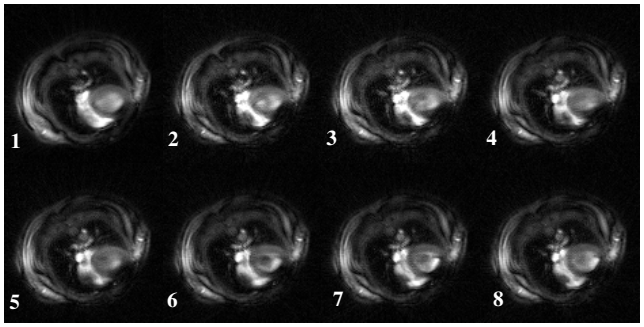

Fig. 5. Radially encoded in vivo mouse cardiac images reconstructed with Toeplitz based maximum likelihood method.

V. ON DENSITY COMPENSATION

To establish the relationship between MNLS formulas and the regular gridding algorithm, we use a consistent matrix form

$$\underline{\mathbf{i}}_{GD} = A^{\dagger} D \underline{\mathbf{s}} \tag{12}$$

for gridding reconstruction, where D is a diagonal density compensation matrix with DCF as its diagonal elements $d_{ii} = d(\mathbf{k}_i)$. In fact, by comparing (4) and (12), we find optimally $D = \left(AA^{\dagger}\right)^{-1}$, which is not necessarily a diagonal matrix. Therefore, gridding method actually approximates matrix $\left(AA^{\dagger}\right)^{-1}$ with its diagonal.

Different from the gridding framework, formula (5) can be interpreted as that operator $A^{\dagger}$ reconstructs the image without density compensation, and operator $\left(A^{\dagger}A\right)^{-1}$ tries to sharpen the resulted blurred image. As opposed to the compensation $\left(AA^{\dagger}\right)^{-1}$ or D in the k-space, $\left(A^{\dagger}A\right)^{-1}$ performs equivalent role but in the image space. However, although matrix $\left(A^{\dagger}A\right)^{-1}$ is also diagonal dominant, it can not be accurately approximated by only its diagonal.

Approximating (5) by (12) with minimized reconstruction error provides alternative solutions for optimal DCFs. First, one could rewrite (5) as

$$\underline{\mathbf{i}}_{ML} = A^{\dagger} A \left(A^{\dagger}A\right)^{-2} A^{\dagger} \underline{\mathbf{s}} \tag{13}$$

and a similar matrix approximation as in [4] will lead to optimal DCF solution

$$d_{ii} = \frac{[A \left(A^{\dagger}A\right)^{-1} A^{\dagger}]_{ii}}{[A^{\dagger}A]_{ii}} \tag{14}$$

Another approach is to equalize (5) and (12) and set $\underline{\mathbf{s}} = \mathbf{1}$, so that we have

$$A^{\dagger}\mathbf{1} = \left(A^{\dagger}A\right) A^{\dagger} d. \tag{15}$$

DCF vector d can be possibly solved with iterative methods. In each iteration, $A^{\dagger}d$ is calculated by NUFFT-2 and $A^{\dagger}A$ operator by FFT/IFFT. Note for both (14) and (15), the density compensation found are generally complex.

VI. CONCLUSIONS

An accurate and fast Toeplitz based maximum likelihood method is developed for non-Cartesian MR image reconstruction. Compared to the gridding method, TML does not need density compensation and thus is applicable to arbitrary k-space trajectory. The simulation studies on radial, spiral, and random sampling patterns showed improved reconstruction accuracy using TML method. The physical phantom scan case also indicated that TML reconstruction resulted in images with higher SNR than gridding reconstruction. The proposed method has also been successfully applied to in vivo cardiac data. The relationship between TML method and gridding algorithm has been revealed and alternative approaches to find optimal DCFs are suggested.

VII. ACKNOWLEDGMENTS

The authors acknowledge the NIH support through grant 5R21CA114680. The MRI scans were performed at the Duke Center for In Vivo Microscopy, an NCRR/NCI national resource (P41 RR005959/R24 CA092656).

REFERENCES

[1] J. O. Sulllivan, "A fast sinc function gridding algorithm for Fourier inversion in computed tomography," *IEEE Trans. Med. Imag.*, vol. MI-4, 1985, pp 200-207.

[2] J. Jackson, C. H. Meyer, D.G. Nishimura and A. Macovski, "Selection of a convolution function for Fourier inversion using gridding," *IEEE Trans. Medical Imaging*, vol. 10, 1991, pp 473-478.

[3] D. Rosenfeld, "An optimal and efficient new gridding algorithm using singular value decomposition," *Mag. Reson. Med.*, vol. 40, 1998, pp 14-23.

[4] H. Sedarat and D. Nishimura, "On the optimality of the gridding reconstruction algorithm," *IEEE Trans. Med. Imag.*, vol. 19, 2000, pp 306-317.

[5] R. Hoge, R. Kwan and G. Pike, "Density compensation functions for spiral MRI," *Mag. Reson. Med.*, vol. 38, 1997, pp 117-128.

[6] C. Meyer, B. Hu, D Nishimura and A. Macovski, "Fast spiral coronary artery imaging," *Mag. Reson. Med.*, vol. 28, 1992, pp 208-213.

[7] V. Rasche, R. proksa, R. Sinkus, P. Bornert and H. Eggers, "Resampling of data between arbitrary grids using convolution interpolation," *IEEE Trans. Med. Imag.*, vol. 18, 1999, pp 385-392.

[8] J. G. Pipe, "Sampling density compensation in MRI: rationale and an iterative numberical solution," *Mag. Reson. Med.*, vol. 41, 1999, pp 179-186.

[9] R. V. de Walle, H. H. Barrett, K. J. Myers, M. I. Altbach, B. Desplanques, and A. F. Gmitro, "Reconstruction of MR Images from Data Acquired on a General Nonregular Grid by Pseudoinverse Calculation," *IEEE Trans. Med. Imag.*, vol. 19, 2000, pp 1160-1167.

[10] R. H. Chan and M. K. Ng, "Conjugate gradiaent methods for Toeplitz systems," *SIAM Rev.*, vol. 38, 1996, pp 427-482.

[11] A. Dutt and V. Rokhlin, "Fast Fourier transforms for nonequispaced data," *SIAM J. Sci. Comp.*, vol. 14, 1993, pp 1368-1393.

[12] Q. H. Liu and N. Nguyen, "An accurate algorithm for nonuniform fast Fourier transform (NUFFT's)," *IEEE Microwave and Guided Wave Letters*, vol. 8, 1998, pp 18-20.

[13] Q. H. Liu and X. Y. Tang, "Iterative algorithm for nonuniform inverse fast Fourier transform (NU-IFFT)," *Electronic Letters*, vol. 34, 1998, pp 1913-1914.

[14] J. A. Fessler, S. Lee, V. T. Olafsson,H. R. Shi,and D. C. Noll, "Toeplitz-Based Iterative Image Reconstruction for MRI With Correction for Magnetic Field Inhomogeneity," *IEEE trans. sig. proc.*, vol. 53, 2005, pp 3393 - 3402.

[15] R. boubertakh, J.-F. Giovannelli, A. De Cesare, and A. Herment, "Non-quadratic convex regularized reconstruction of MR images from spiral acquisitions," *Signal Processing*, in press.

[16] J. Song and Q. H. Liu and S. L. Gewalt and G. P. Cofer and G. A Johnson, "General least square NUFFT methods applied to 2D and 3D radially encoded MR image reconstruction," *IEEE Trans. Med. Imag.*, 2006, submitted.